

Fast Equilibrium Micro-Extraction from Biological Fluids with Biocompatible Core–Sheath Electrospun Nanofibers

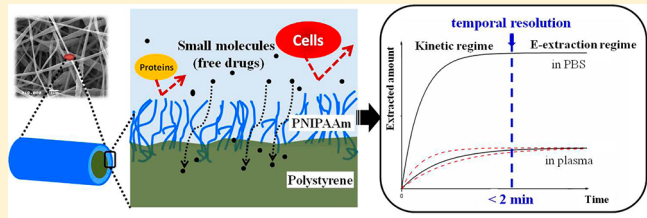
Qian Wu,^{†,‡} Dapeng Wu,^{*,†} and Yafeng Guan^{*,†}

[†]Department of Instrumentation and Analytical Chemistry, Key Laboratory of Separation Science for Analytical Chemistry of CAS, Dalian Institute of Chemical Physics, Chinese Academy of Sciences, 457 Zhongshan Road, Dalian 116023, P. R. China

[‡]Dalian Institute of Chemical Physics, Graduate School of the Chinese Academy of Sciences, Beijing 100039, P. R. China

Supporting Information

ABSTRACT: Sample preparation methods with high temporal resolution and matrix resistance will benefit fast direct analysis of analytes in a complex matrix, such as drug monitoring in biofluids. In this work, the core–sheath biocompatible electrospun nanofiber was fabricated as a micro-solid phase extraction material. With the poly(*N*-isopropylacrylamide) (PNIPAAm) as sheath polymer and polystyrene (PS) as core polymer, the fiber membrane was highly hydrophilic and exhibited good antifouling ability to proteins and cells. Its complete expansion in aqueous solution and its nanoscale fiber (100–200 nm) structure offered high mass transfer rate of analytes between liquid and solid phases. The equilibration time of microextraction with this membrane was all shorter than 2 min for eight drugs tested, and the linear ranges covered more than 3 orders of magnitude for most of them. This membrane could be applied to monitor free drugs in plasma and their protein binding kinetics by equilibrium–microextraction with a 2 min temporal resolution. The results showed that the core–sheath electrospun nanofiber membrane would be a better alternative of solid phase material for microextraction with good matrix-resistance ability and high temporal resolution.



Temporal resolution and matrix resistant ability are always two key factors in bioanalysis, such as drugs monitoring for pharmacokinetics, short-lived intermediate metabolites analysis, and a protein binding kinetics study of drugs in a biological system.¹ During most of the analytical process, sample preparation is the critical and the most time-consuming step. Thus, the development of a rapid and matrix resistant sample preparation method, both *in vivo* and *in vitro*, is essential for bioanalysis.

Solid phase extraction (SPE) is a widely used sample preparation method. However, as an exhaustive extraction method,² SPE usually would deplete the sample, which does not meet the basic requirements of some biosample monitoring^{1a,b} and *in vivo* analysis³ that the extraction process should not significantly disturb the biosystem balance. In the early 1990s, Pawliszyn and co-workers developed solid phase microextraction (SPME),⁴ which was a nonexhaustive method and could avoid this problem.³ However, the matrix effect of biosamples would still result in two problems. First, due to the complicated matrix in a biological system, the extraction phase would get fouled and changed from their primary extraction behavior.^{5,6} Second, biomatrix would change the mass transfer kinetics of analytes among samples, which would limit the use of pre-equilibrium extraction (PE-extraction) with external standard calibration.^{1c,7} However, for most of the extractive materials,⁸ equilibrium extraction (E-extraction) requires long extraction time due to slow mass transfer kinetics, which decreases the temporal resolution of bioanalysis. Internal

standard calibration could not provide the free concentration of analytes and is not suitable for *in vivo* extraction.^{3,8c}

In recent years, biocompatible extractive materials, such as restricted access materials (RAM),^{8b} PPY,⁹ or common extraction phases with biocompatible polymers as covering layers,^{8c,10,11} were introduced into SPME to avoid the first problem and applied to bioanalysis, such as *in vivo* free drug extraction. However, the second problem was still reserved in SPME. The reported fastest E-SPME was a 2 min extraction with a 10 μm polypyrrole (PPY) coating,⁹ but the thin porous PPY coating exhibited low extraction capacity. Other biocompatible SPME coatings with high extraction capacity, such as RAM sorbents, C18–polyacrylonitrile coating, and C18–poly(ethylene glycol) coating could not have a fast enough mass transfer rate providing a high temporal resolution for E-extraction.^{8c,9,10} To increase the temporal resolution of SPME, PE-extraction was used, and a kind of kinetic calibration was developed to compensate variation in sampling kinetics caused by biomatrix.¹² However, PE-extraction usually gets low sensitivity and requires accurate timing.^{3,13,14} Kinetic calibration usually needs deuterated standards preloaded on the solid phase¹⁵ and needs the distribution coefficients of analytes between phases to calculate the results,^{1c,10a,15} which would complicate the whole calibration process. Moreover, free

Received: March 7, 2013

Accepted: May 23, 2013

Published: May 23, 2013



concentration of analytes in biofluids, such as blood, could not be measured directly by using kinetic calibration without the binding constant of the drugs to the blood matrix.^{8c,10a} Thus, a biocompatible extractive material with a fast enough mass transfer rate to ensure high temporal resolution of E-extraction is still favored and needed in current bioanalysis.

Enlightened by studies of extractive material with rapid mass transfer kinetics,^{9,10} we for the first time introduced a kind of core–sheath electrospun nanofiber as the extractive material for micro-SPE. Electrospun nanofiber¹⁶ recently has been applied to SPE and SPME due to its large surface area.¹⁷ In this work, poly(*N*-isopropylacrylamide) (PNIPAAm) as a well-known biocompatible¹⁸ and protein-resistant¹⁹ polymer was used as the sheath of core–sheath electrospun nanofiber, and polystyrene (PS) as a widely used extractive material²⁰ was used as the core. The PNIPAAm sheath not only provided a biomatrix resistance of the extractive material but also ensured a complete and fast expansion of the nanofibers in aqueous phase, which can be expected to provide more rapid mass transfer kinetic without loss of extraction capacity. In addition, the integrity of the fiber material makes it easy to separate from sample after extraction,^{17a,c,20} which is a unique merit compared with other functional nanoparticles or packing microbeads.²¹ The biocompatible extractive material was then used to extract free drugs in biological samples. Good biomatrix antifouling property as well as high mass transfer rate of target drugs (equilibration time <2 min) and wide linear ranges (more than 3 orders of magnitude) was obtained. Finally, it was used to measure plasma protein binding constants and protein binding kinetics of different drugs by the E-microextraction method.

■ EXPERIMENTAL SECTION

Chemicals and Materials. Amitriptyline (95% pure) were purchased from Sigma–Aldrich Co. (St. Louis, MO, USA). Propranolol (95% pure) was purchased from Acros Organics (Morris Plains, NJ, USA). Desipramine (95% pure) and berberine chloride (95% pure) were purchased from J&K Scientific Ltd. (Beijing, China). Four intermediates of drug synthesis (see the structures in Figure S1, Supporting Information, named I1, I2, I3, and I4) were provided by Jiangsu Vcare Pharmatech. Co. (Nanjing, China). Bovine serum albumin (98%) was purchased from Jingke reagent Co. (Beijing, China). 2,5-Dihydroxybenzoic acid (2,5-DHB) and sinapinic acid (SA) were obtained from Sigma (St. Louis, MO). NaH₂PO₄ and NaOH (analytical grade) used to prepare phosphate buffer saline (PBS, pH = 7.4) were bought from Shenyang Chemical Reagent Co. (Shenyang, China). PS (M_w = 250 000–270 000, general type I) was purchased from Aladdin industrial Co. (Shanghai, China), and PNIPAAm (M_w = 19 000–26 000) was purchased from Sigma–Aldrich Co. (St. Louis, MO, USA). Dimethylformamide (DMF), tetrahydrofuran (THF), and chloroform were obtained from Kermel Chemical Reagent Co. (Tianjing, China). The materials were used without any purification. Acetonitrile and methanol of HPLC grade were purchased from Merck Co. (Darmstadt, Germany). Human plasma of health adults was obtained from the Second Affiliated Hospital of Dalian Medical University.

Preparation of Electrospun Fibers. 10% (w/v) PS/PNIPAAm (1:1, w/w) solution in DMF/chloroform (2:5, v/v), 10% (w/v) PS/PNIPAAm (1:1, w/w) solution in THF, and 10% (w/v) PS solution in DMF/THF (3:7, v/v) were prepared at room temperature and stirring for 5 h, respectively. Syringe pump (LSP01-1, Longerpump, Baoding, China) and an

electrode of high voltage power supply (ADW300-0.5, Dongwen high voltage power supply factory, Tianjing, China) was clamped to the metal needle tip. The flow rate of polymer solution was 1 mL h⁻¹, and the applied voltage was 18 kV. The tip-to-collector distance was set to 12 cm, and a grounded aluminum foil (15 cm × 20 cm) cover was used for the fiber collection. The humidity during electrospinning is kept within 45–60%.

Measurements and Characterization. After a 1 min gold sputtering, the fiber morphology was examined by scanning electron microscopy (SEM) (JSM 6360, Japan) at 20 kV. The nanofibers were examined by a transmission electron microscope (TEM, JEM-2000EX). For the preparation of TEM samples, the nanofibers were collected on a carbon coated copper specimen grid.

X-ray photoelectron spectroscopy (XPS) was performed using a multitechnique ultrahigh-vacuum imaging XPS microprobe system (Thermo ESCALAB 250Xi) equipped with a monochromated Al KR X-ray source ($h\nu$ = 1486.6 eV) operating at 15 kV and 14.9 mA. The detailed information is summarized in Method S1, Supporting Information.

The contact angle (CA) was measured by system JC 2000A (Powereach Ltd, Shanghai, China) with water droplets of 2 μ L for 2 min and repeated five times. It was confirmed that the CA had reached the equilibrium values in 2 min according to the time profiles of the CA (Figure S2, Supporting Information).

MALDI-TOF mass analysis results were obtained by a tandem time-of-flight (TOF/TOF) mass spectrometer (5800 system, AB SCIEX, USA). The detailed information is summarized in Method S2, Supporting Information.

Extraction Procedure. Stock solutions of 1 mg mL⁻¹ investigated drugs were prepared in methanol and kept at -20 °C as well as human plasma until analysis. For analysis, plasma was thawed at room temperature and transferred into clean vials. Appropriate amounts of drug standards were added in plasma samples and PBS (12 mmol L⁻¹, pH 7.4) to obtain final concentrations in the range of 0.1–1000 ng mL⁻¹, followed by vortex mixing for 30 min.

For fast free drug analysis, 2.5 mg of extracting phase of electrospun fibers was put into the samples (1 mL) placed on a temperature controlled shaking bed (SHZ-82A, Weier experimental equipment Ltd, Suzhou, China) for a precise period of time. After extraction, the fiber was then briefly rinsed with water and then centrifuged at 4000 rpm for 1 min to remove the excess water in the fibers. Dried fibers were desorbed in 50 μ L of 80% methanol–water solution for 10 min without stirring (desorption time was chosen according to Figure S3, Supporting Information). Two μ L of desorption solution was introduced to LC-MS/MS for analysis.

For investigation of drug–protein binding kinetics, 50 mL of 1 mg mL⁻¹ BSA solution and 50 mL of 10 ng mL⁻¹ eight drug solution were prepared in PBS in two separate 100 mL beakers stirred for 30 min at room temperature. At time t = 0, 50 mL of BSA solution was mixed with the 50 mL of drug solution (under constant stirring at 600 rpm), and fiber mat was introduced into the sample for a precise 2 min sampling duration at t = 1, 4, 8, 12, 16, 20, 24, 28, 32, 36, 40, 44, 48, 52, and 56 min. After extraction, the fibers were rinsed, centrifuged, and desorbed similarly to the fast free drug analysis.

LC-MS/MS System. For HPLC-MS/MS analysis, an Agilent 1200 series HPLC system (Agilent Technologies, USA), consisting of a binary pump, vacuum degasser, autosampler, and column temperature controller, coupled

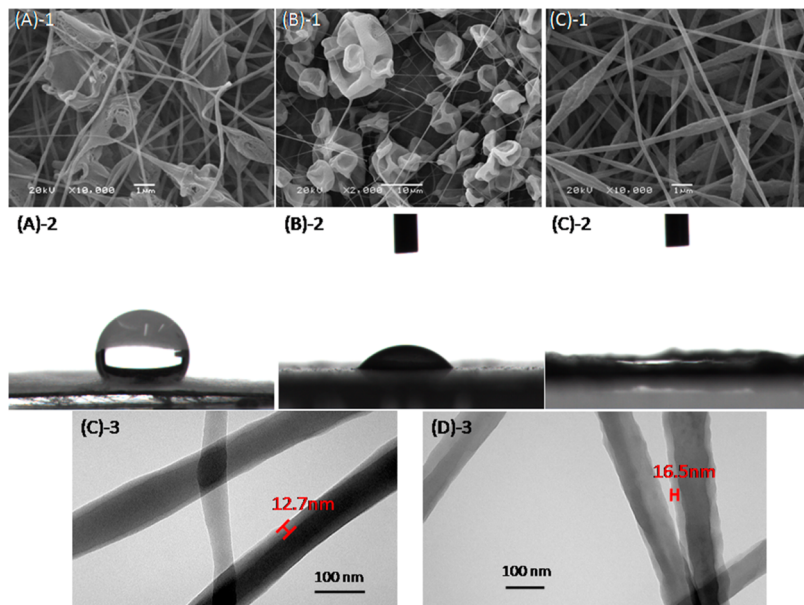


Figure 1. SEM images (1) and water contact angles (2) of PS (A), conventional PS/PNIPAAm composite (B), and core–sheath PS/PNIPAAm composite (C) electrospun fibers and TEM images (3) of core–sheath PS/PNIPAAm composite electrospun fibers before (C) and after (D) 1 h of water washing.

with a Agilent 6460 triple quadrupole mass spectrometer, was used for the identification and quantification. A C18 column (Agilent ZORBAX SB-C18, 50 mm × 2.1 mm, 1.8 μm) was used for separation. The mobile phase for separation of eight target analytes was a linear gradient of 20–90% acetonitrile in an aqueous solution with 0.05% formic acid during 10 min following a 5 min constant elution of 90% acetonitrile at 0.2 mL min⁻¹ flow rate. The parameters of MS/MS detection are summarized in Table S1, Supporting Information.

RESULTS AND DISCUSSION

Preparation of Core–Sheath Electrospun Fibers. According to the mechanism of single-spinneret electro-

Table 1. Surface Composition of Core–Sheath PS/PNIPAAm Nanofibers

		method a ^a	method b ^b	method c ^c
before washing	%PNIPAAm	82%	81.9%	81.5%
	%PS	18%	18.1%	18.5%
after washing	%PNIPAAm	57%	62%	61.7%
	%PS	43%	38%	38.3%

^aMethod a: %PNIPAAm = 8/([C]/[N] + 2). ^bMethod b: %PNIPAAm = (6[C–C]/[C=C] – 2)/(6[C–C]/[C=C] + 2).

^cMethod c: %PNIPAAm = 2/([C–C]/[C–N] – 2).

spinning of core–sheath nanofibers reported by Chen and co-workers,²² the PNIPAAm/PS mixture in two mixed solvents were electrospun. The two solvents were required to have a large difference in boiling point and in solubility of two polymers, so chloroform and DMF were used. Thin and uniform core–sheath composite fibers (100–380 nm, Figure 1(C-1)) had been prepared and were compared with unitary PS fibers (100–200 nm, Figure 1(A-1)) and PNIPAAm/PS composite fibers electrospun with unitary solvent (THF) (Figure 1(B-1)). It can be seen that many more beads appeared when unitary solvent was used in composite fiber (Figure 1(B-1)). These beads would decrease the mechanical

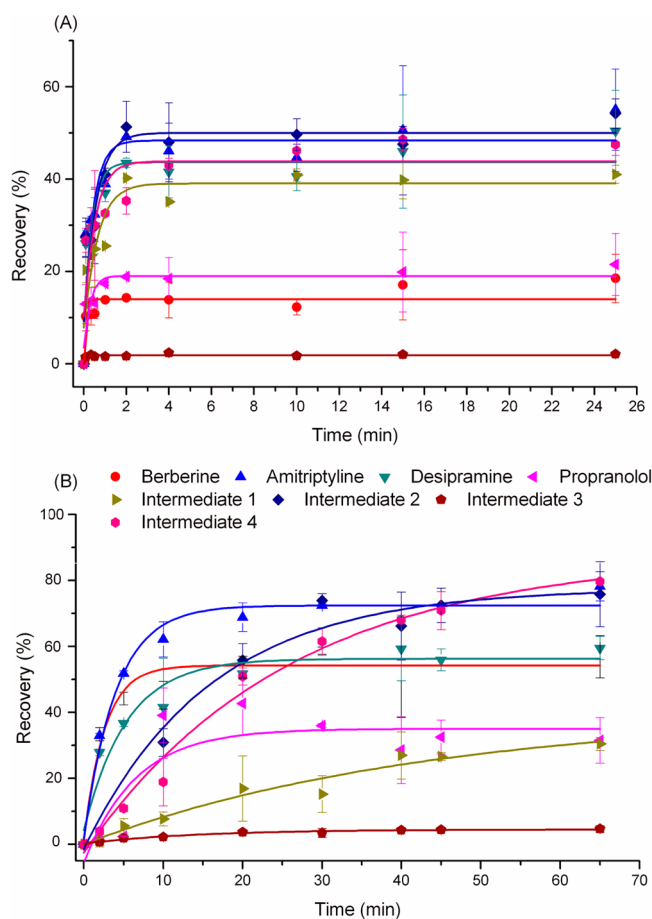


Figure 2. Time profiles of microextraction recovery with core–sheath PS/PNIPAAm nanofibers (A) and PS nanofibers (B) ($n = 3$).

strength of fibers. Thus, besides the formation of core–sheath structure, binary solvent could also suppress the formation of beads in the fibers and help form thinner uniform fibers.

Table 2. Comparison of Thermodynamic and Kinetic Parameters of Extraction with PS Nanofibers and Core–Sheath PS/PNIPAAm Nanofibers

drugs	<i>K</i>		<i>v</i> (cm ³ min ⁻¹)	
	PS/PNIPAAm	PS	PS/PNIPAAm	PS
berberine	7.93×10^1	1.08×10^2	1.55×10^{-2}	1.65×10^{-4}
amitriptyline	4.99×10^2	4.50×10^2	1.25×10^{-3}	1.44×10^{-4}
desipramine	2.73×10^2	2.24×10^2	1.95×10^{-3}	1.17×10^{-4}
propranolol	1.08×10^2	6.60×10^1	3.39×10^{-3}	4.43×10^{-3}
intermediate 1	2.64×10^2	5.70×10^1	1.17×10^{-3}	2.33×10^{-5}
intermediate 2	5.68×10^2	1.68×10^3	9.03×10^{-4}	2.50×10^{-5}
intermediate 3	4.55×10^1	2.90×10^1	1.86×10^{-2}	7.72×10^{-5}
intermediate 4	9.18×10^2	1.25×10^3	7.17×10^{-4}	1.85×10^{-5}

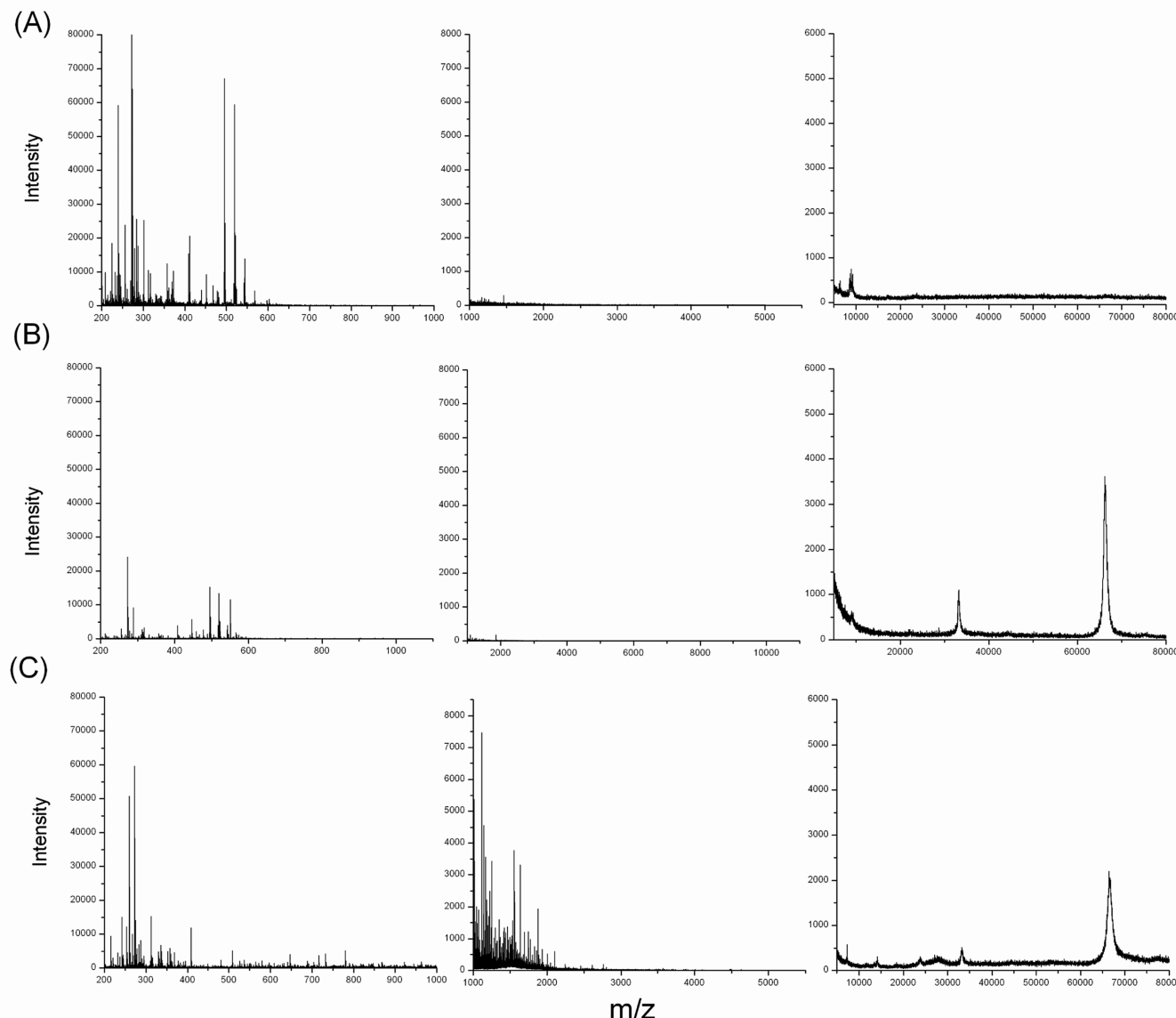


Figure 3. MALDI-TOF MS analysis of human plasma after treatment by PS/PNIPAAm core–sheath fibers (A), unitary PS fibers (B), and C18 sorbents (C).

Surface enrichment of PNIPAAm on composite fiber, which demonstrated its core–sheath structure, was confirmed by XPS quantification and TEM. According to the wide energy survey scans result (Figure S4(A), Supporting Information), the surface coverage of PNIPAAm (%PNIPAAm) can be calculated

from the [N]/[C] value of the surface. On the other hand, from the C1s core-level spectrum (Figure S4(B), Supporting Information), %PNIPAAm can also be calculated from the ratio between different hybridized carbons. From Table 1, it can be seen that %PNIPAAm on the surface was around 82% from

Table 3. Analytical Performance of Eight Drugs Analysis

drugs	standard				plasma				15% plasma			
	linear range ^a (ng mL ⁻¹)	slope ^b	R ²	RSD ^c	linear range ^a (ng mL ⁻¹)	slope ^b	R ²	RSD ^c	linear range ^a (ng mL ⁻¹)	slope ^b	R ²	RSD ^c
berberine	0.5–100	3.01 × 10 ³	0.9999	9%	1–1000	2.80 × 10 ²	0.9952	10%	0.5–500	5.69 × 10 ²	0.9999	17%
amitriptyline	0.1–500	9.52 × 10 ³	0.9992	4%	0.25–1000	1.25 × 10 ³	0.9900	10%	0.25–1000	2.19 × 10 ³	0.9980	10%
desipramine	0.1–500	1.22 × 10 ⁴	0.9998	5%	0.1–1000	1.13 × 10 ³	0.9999	11%	0.25–500	5.89 × 10 ³	0.9996	3%
propranolol	0.25–100	9.19 × 10 ²	0.9999	12%	0.25–1000	3.10 × 10 ²	0.9900	10%	1–500	6.05 × 10 ²	0.9998	16%
intermediate 1	0.1–100	2.74 × 10 ⁴	0.9997	8%	1–1000	3.12 × 10 ³	0.9918	4%	0.1–500	1.25 × 10 ⁴	0.9981	7%
intermediate 2 ^d	0.5–1000	9.50 × 10 ¹	0.9997	4%					1–1000	1.60 × 10 ¹	0.9924	14%
intermediate 3	0.5–500	4.27 × 10 ³	0.9970	4%	0.5–500	2.99 × 10 ³	0.9950	11%	0.5–500	3.48 × 10 ³	0.9993	10%
intermediate 4	0.25–1000	1.32 × 10 ³	0.9998	4%	0.25–1000	2.70 × 10 ²	0.9918	10%	0.1–500	1.31 × 10 ³	0.9940	7%

^aCalibration standards concentrations were shown in Figure S9, Supporting Information. ^bThe fitting calibration curves were shown in Figure S9, Supporting Information. The fitting expression is: $y = ax + b$. x is the concentration of analytes in the sample (ng mL⁻¹), and y is the peak area of analytes in sample after extraction. ^cRepeated for three times. ^dIntermediate 2 was not detected in pure plasma because of its low free concentration in plasma and low MS response.

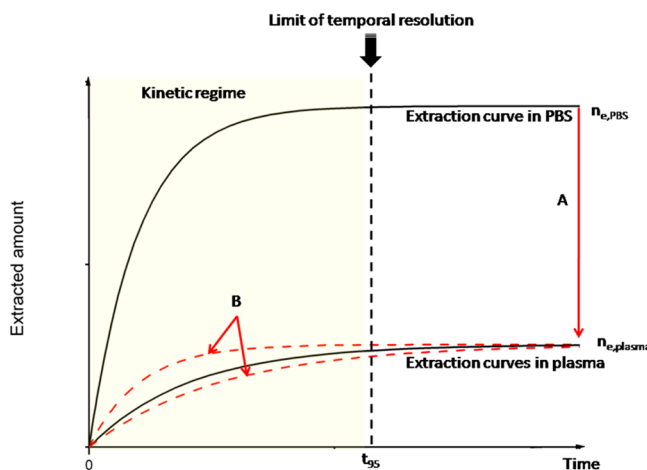


Figure 4. Illustration of matrix effect on solid phase extraction.

Table 4. Experimental and Literature Drug Plasma Protein Binding Values

plasma protein binding %	plasma	15% plasma	literature value ^a
berberine	90.6%	81.1%	88%
amitriptyline	86.8%	76.9%	80%
desipramine	90.7%	51.5%	82%
propranolol	66.3%	34.2%	63–74.9%
intermediate 1	88.6%	54.3%	
intermediate 2		83.1%	
intermediate 3	29.8%	18.5%	
intermediate 4	79.5%	0.53%	

^aReference 26.

all the methods, which demonstrates that the surfaces (uppermost 10 nm in depth²³) were enriched with PNIPAAm. From the TEM (Figure 1(C-3)), the sheath structure can be seen clearly to be 12 nm thick by the different lightness of polymers caused by their different electron transmissivities.

The electrospun fibers exhibited excellent hydrophilicity property. From Figure 1(A-C)-2 and Figure S2, Supporting Information, the equilibrium water CA of core–sheath fibers was about 0° at room temperature, while that of composite fibers electrospun with unitary solvent is just 60° at room temperature. The better hydrophilicity is of great help to the protein/cells antifouling property as well as acceleration of extraction due to the well wetting (Figure 1(C)-2) and fast

expansion of material in aqueous sample with good integrity (Figure S5(E–G), Supporting Information), which will be discussed in detail in the next sections.

The stability of fibers in water had also been investigated, as shown in Figure S5, Supporting Information. It can be seen that fibers would have a weight loss (~30%) during a 5 min rinse in water, but for a longer time (>20 min) of washing, the weight loss was minimized. It may be caused by dissolving solvent residue and polymer impurities in fibers or the gradual bleeding of PNIPAAm from the fibers as reported.²⁴ To ensure the morphology and core–sheath structure of fibers kept well after washing, SEM of fibers with 1 h and 14 h of washing and TEM and XPS of fibers with 1 h of washing were carried out (Figure S5, Supporting Information, Figure 1(C-4) and Table 1). The results showed that the core–sheath structure could be well maintained after water washing though the weight loss was detected, but the swelling of the sheath and decrease of PNIPAAm content could not be avoided. Finally, the effect of water washing on extraction efficiencies was investigated, and it can be seen (Figure S6, Supporting Information) that the extraction recoveries were lower for some drugs with water washed fibers. Fortunately, the decrease of recoveries were at a minimum after 20 min of washing. All the information indicated that the core–sheath structure was kept well and became stable after 20 min water washing. Thus, to stabilize fibers for extraction, they should be washed 1 h before use.

Fast and Direct Micro-Extraction by Biocompatible Core–Sheath Fibers. *Kinetic Consideration.* The extraction time profiles of eight model drugs using core–sheath PNIPAAm/PS composite fibers and PS fibers were shown in Figure 2. The experimental value of equilibration time (ET) was conveniently expressed as the time required to extract 95% of the equilibrium amount of analytes. From Figure 2, it can be seen that the ET was less than 2 min for all the drugs (500 μL sample) using composite fibers but was 10–60 min using PS fibers.

According to the mass transfer kinetic theory,^{14,15} the extraction time profiles can be simulated as

$$\frac{n}{n_e} = 1 - e^{-at} \quad (1)$$

$$a = \frac{A\beta}{V_s} \left(\frac{KV_s}{V_a} + 1 \right) \quad (2)$$

$$v = A\beta \quad (3)$$

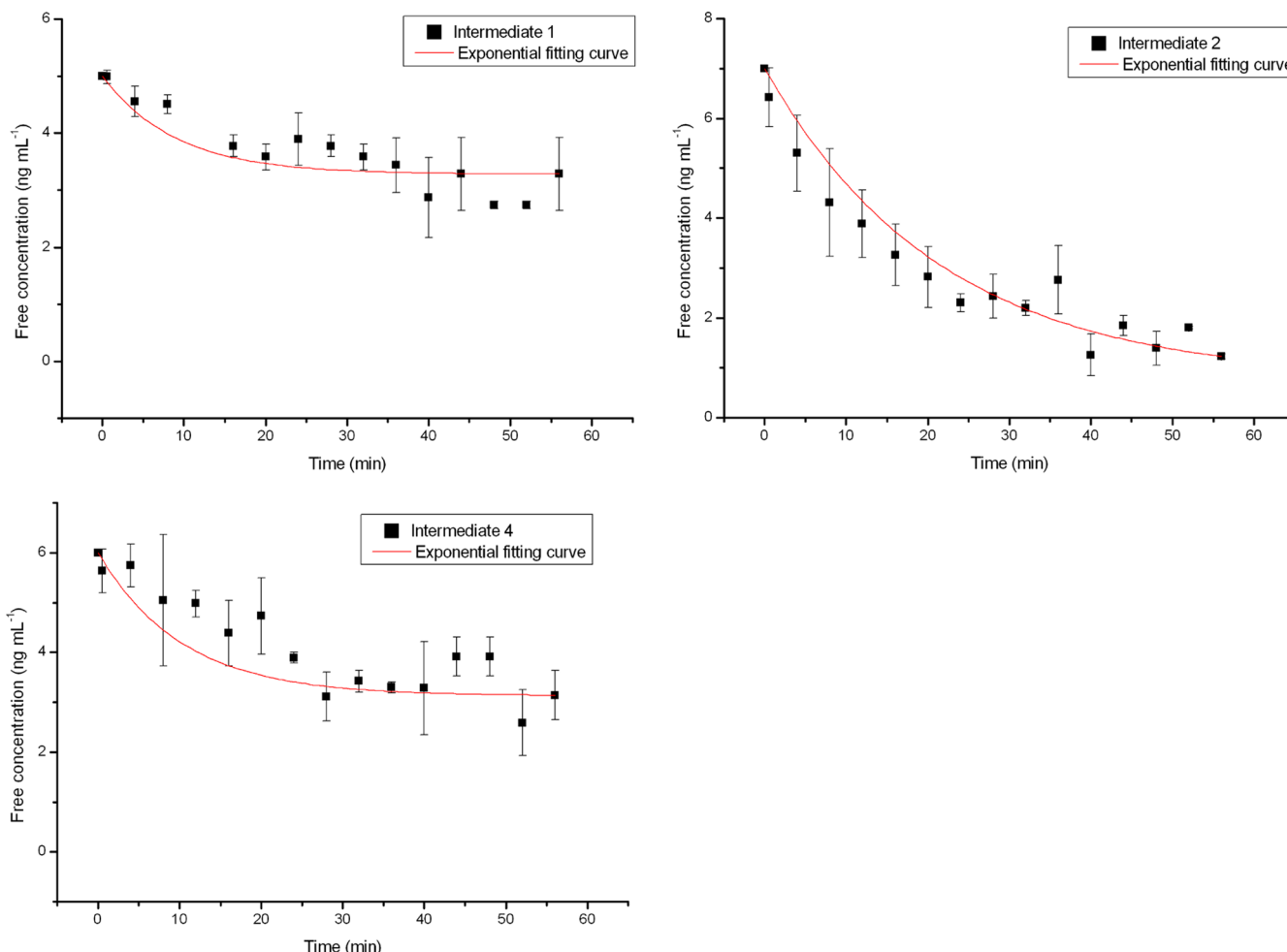


Figure 5. Temporal changes in the free concentrations of three drugs as determined by core–sheath nanofiber equilibrium microextraction after introduction of BSA protein ($n = 3$).

where n_e is extracted amount of analyte at equilibrium, n is that at time t , a is the time constant of extraction, V_a is the aqueous phase volume, V_s is the solid phase volume, A is the interface area between two phases, K is the distribution constant (DC) of analytes between two phases, and β is the mass transfer coefficient of analytes. From the equations, it can be seen that ET is related to a lot of conditions of extraction (such as V_a , V_s , and K), so the essential parameter (ν) for mass transfer kinetic, which is only related to A and β , was calculated to compare the two materials. ν can be calculated by fitting the extraction time profile to eqs 1 and 2 (Table 2). It can be seen that ν of extraction with composite nanofibers was at least ten times of that with PS nanofibers.

The much higher ν value could be related to A and β from eq 1, and β is highly related to the diffusion coefficients of analytes (D) and the thickness of diffusion layer (δ).¹⁴ Except D , other two terms (A and δ) are in close relation to the features of solid phase material. As to A , it is determined by the solid surface areas of the extraction phase, the wetting state in the sample solution. Though the electrospun nanofibers obviously have large surface area due to its small diameter of fibers, the hydrophobic PS nanofibers of low surface energy will congregate seriously or trap air in it resulting in a significant decrease of interfacial area with water. On the contrary, composite PNAIAAm/PS fibers with sheath hydrophilic layer would be easily wetted, expanded in aqueous solution

completely, and exhibited a much larger A . As to δ , it could be divided into two parts for most solid phases.^{14,15} One is the diffusion layer in the aqueous phase adjacent to the interface (δ_1), and the other is that in porous PS electrospun fibers (δ_2). δ_1 is commonly in the level of a micrometer with stirring in the sample,⁷ and δ_2 depends on the fiber diameter and the pore structure. Because of the smaller diameter of core–sheath fibers (100–400 nm), its δ_2 is significantly decreased to hundreds of nanometers. Moreover, unlike other modified biocompatible SPME coatings with micrometer level hydrophilic polymer layer,^{8c,10a} δ_1 of core–sheath fibers will not be significantly increased by the thin biocompatible sheath layer (10–20 nm). On the basis of the above-mentioned consideration, the strong hydrophilic and nanometer level sheath layer is a crucial factor for the ultra fast mass transfer of composite fibers.

Equilibrium Consideration. For static extraction with solid phase from aqueous phase, DC can be calculated as:⁴

$$K = \frac{n_e V_a}{V_s (C_0 V_a - n_e)} \quad (4)$$

where C_0 is the initial concentration of a given analyte in the sample.

For DC measurements, 12 mM PBS (pH = 7.4) was used as the sample buffer. It can be found that DC was similar with two solid phases (PS fibers and core–sheath PS/PNIPAAm fibers) for most of the drugs, but the hydrophilic drugs had higher DC

with core–sheath fibers, and hydrophobic drugs had higher DC with PS fibers (Table 2). This phenomenon indicated that the PNIPAAm also has a little effect on the extraction behavior of the core. The hydrophilic PNIPAAm layer could increase the polarity of the solid phase and increase the distribution of polar drugs.

Capability of Bio-Matrix Resistance. To demonstrate the antifouling ability of the core–sheath fibers to proteins and peptides, MALDI-TOF was used to detect the human plasma sample after core–sheath fibers, PS fibers, and C18 sorbents pretreatment (Figure 3, Method S3, Supporting Information). In Figure 3, molecules larger than 600 Da were extracted minimally for core–sheath fibers, which meant most of the peptides and proteins could be excluded effectively. It was due to the formation of a strong hydration layer by PNIPAAm, which prevents intimate molecular contact between proteins and fiber surface,^{18b,19c} and the size exclusion effect of the dense sheath layer to proteins and peptides. However, PS fibers showed no obvious proteins or peptides resistance ability (Figure 3(B)).

To demonstrate the antifouling ability of core–sheath fibers to cells, microscopic pictures of fibers after exposure to whole blood had been taken (Figure S7, Supporting Information). It can be seen that the blood cell attachment of the composite fibers was negligible, while that of PS fibers was obvious.

Other small molecules coextracted with drugs could still affect the MS response by matrix-induced ionization suppression/enhancement. The results of PS fibers and core–sheath fibers were compared. As shown in Figure S8, Supporting Information, matrix effect was evaluated by the relative response (RR) of matrix-matched standards to matrix-free standards after extraction (see Method S4, Supporting Information),^{1d} and RRs of all drugs were from 90% to 120% with core–sheath fibers as extractive material but varied from 50% to 130% for PS fibers. Thus, the coextracted matrix with core–sheath fibers was negligible to affect the LC-MS/MS responses of target drugs.

Reproducibility of Microextraction and Reusability of the Fibers. Standard drug solution in PBS only, diluted plasma (15%), and plasma solutions were extracted for three times by three composite fiber mats (2.5 mg each) for 2 min. The reproducibilities were all below 10% (Table 3). Moreover, from the extraction time profiles with core–sheath fiber mats (2.5 mg each), it could be seen that the relative standard deviations (RSDs) were all below 20% at extraction time before equilibrium (Figure 2).

To investigate reusability of the fibers, free fiber mats were used for repeated extractions from human plasma (Figure S9, Supporting Information). Extraction efficiencies changed little after five extractions and desorptions, but the RSDs increased dramatically (from <10% to 40–70%) for some drugs after three extractions. This may be due to the instability of the sheath layer and the accumulated carry-over on the fibers after long time extraction, desorption, and washing. Since sample preparation devices for biological samples are generally of single use, we used the fibers only once in all our experiments.

Application to Free Drugs Analysis in Bio-Samples. When a static extraction method with solid phase as extractive phase was applied to biological analysis, n_e would change among different samples (A in Figure 4) due to serious surface fouling of extractive materials.^{5,6} In addition, the mass transfer kinetic and extraction time profile before equilibrium would deflect (B in Figure 4), which makes PE-extraction less accurate

for calibration.^{1c,7} Fortunately, the proposed core–sheath fiber has shown high antifouling ability that can avoid the change of n_e and separate the small molecules from biomatrix. Moreover, its high mass transfer rate ensured its E-extraction with high temporal resolution. Thus, it is very suitable for free drugs monitoring in biological samples^{8c} and study of protein binding kinetics of pharmaceuticals.²⁵

Fast Free Drug Analysis in Plasma. The extraction time profiles of eight drugs in plasma and in PBS were first investigated with both core–sheath fibers and unitary PS fibers. As shown in Figure S10, Supporting Information, the matrix effect changed the mass transfer rate of analytes significantly, especially for PS fibers as extractive material. From Figure S10, Supporting Information, it can be seen the quantification results of free drugs with PS fibers were various at different extraction times before ET. However, when ET was short and E-extraction could be used (as the results of PNIPAAm/PS composite fibers), the results were not related to the mass transfer kinetic, so the quantification results were identical at different extraction times (Figure S10, Supporting Information). Thus, E-extraction with core–sheath fibers could obtain more accurate results with higher temporal resolution.

2.5 mg fibers for each 1 mL sample were used to extract free drug with different concentration levels for 2 min E-extraction from standards solution in PBS, diluted plasma (15%), and plasma solutions. As shown in Table 3, a very good linear relationship ($r^2 > 0.99$) was obtained for a seven or eight point calibration ($n = 3$), and the linear range covered 3–4 orders of magnitude for all the drugs both in plasma and PBS buffer. It was also found in Figure S11, Supporting Information, that drug binding to plasma proteins changed the amount of free drug available for extraction and resulted in different calibration slopes and linear ranges for plasma and PBS. The larger slope of diluted plasma (15%) than plasma also demonstrated the dilution of plasma could much favor the release of drugs from proteins.²⁰

Determination of Drug Plasma Protein Binding. Measuring of the amount of drugs binding to plasma proteins is very critical in drug discovery and development. According to previous studies,^{8c} the percentage of drug binding to plasma proteins (%B) could be calculated by eq 4, expressed as

$$\%B = \frac{C_{\text{total}} - C_{\text{free}}}{C_{\text{total}}} \times 100 = \left(1 - \frac{\text{slope}_{\text{plasma}}}{\text{slope}_{\text{PBS}}} \right) \times 100 \quad (5)$$

where C_{total} is the total concentration of drug in plasma, C_{free} is the free concentration of drug in plasma, and $\text{slope}_{\text{plasma}}$ and $\text{slope}_{\text{PBS}}$ are the slopes of the drug calibration curve in plasma and PBS, respectively. Equation 5 was applied for the determination of %B for the eight test drugs, and the results were summarized in Table 4. Literature values of some drugs' %B have also been listed in Table 4, and it can be seen that the experimental values were close to the literature values.²⁶

Studying the Protein Binding Kinetics of Pharmaceuticals. To demonstrate the capability of fast E-extraction with core–sheath nanofibers to track rapid binding kinetics, BSA binding kinetics of target drugs was investigated by this method. According to previous studies,²⁵ the mass-uptake model of microextraction in a dynamic system can be deduced as eq 6. When E-extraction is carried out, eq 5 could approximately be equal to eq 7.

$$n = (C_0 - b/a)V_s K(1 - e^{-at}) + V_s Kbt \quad (6)$$

$$n = C_0 V_s K + (bt - b/a)V_s K \quad (7)$$

where b is the concentration change rate in sample.

ET in this experiment was calculated to be around 2 min by substituting eq 1 with parameters in Table 2 and conditions of this experiment. To determine the real-time concentration, the second term in eq 7 should be insignificant relative to that from the initial concentration (less than 5% of the first term), and time constant a in our system can be calculated to be at least 0.025 (s^{-1}) from extraction time profiles of analytes, so sampling time should be in the range of $120 \sim ((C_0)/(20b) + 40)$ (s). Thus, the temporal resolution of this extraction method was only suitable for the dynamic system with b smaller than $0.0375C_0$ (min^{-1}). According to this restriction and our pre-experiments, only three drugs were suitable for tracking rapid binding kinetics (the results of other five drugs are in Figure S12, Supporting Information), and we used 2 min as the extraction time. The time profile of free drugs in BSA solution analyzed by this method was shown in Figure 5. It can be seen that the time profiles were fitted by exponential fitting, and the good fitting results demonstrated that BSA binding reaction was a pseudofirst-order reaction, which agreed well with previous study.²⁵

CONCLUSION

Hydrophilic and biocompatible core–sheath PS/PNIPAAm composite nanofiber membrane was fabricated and characterized. The membrane was used as the solid phase material for E-microextraction of free drugs in plasma sample. The high mass transfer rate and good matrix-resistance capability of this material had been demonstrated, and E-microextraction with the nanofiber membrane was applied to investigate plasma protein binding percentage of eight drugs and BSA-drug binding kinetics successfully. The biocompatibility of this material and high temporal resolution of extraction with this material showed its great potential to be used as in vivo extraction solid phase for a live biological system. To realize its application to in vivo extraction, further research will be focused on the stability of the nanoscale biocompatible layer and mechanical strength of the fibers.

ASSOCIATED CONTENT

Supporting Information

Methods S1–S4, Figures S1–12, and Table S1. This material is available free of charge via the Internet at <http://pubs.acs.org>.

AUTHOR INFORMATION

Corresponding Author

*E-mail: guanyafeng@dicp.ac.cn (Y.G.).

Notes

The authors declare no competing financial interest.

ACKNOWLEDGMENTS

The financial support by the National Nature Science Foundation of P. R. China (Grant Nos. 90917020, 21005080, 21275144) is gratefully acknowledged.

REFERENCES

- (1) (a) Musteata, F. M. *Bioanalysis* 2009, 1 (1), 171–185.
- (b) Musteata, F. M. *Bioanalysis* 2011, 3 (15), 1753–1768.
- (c) Zhang, X.; Oakes, K. D.; Hoque, M. E.; Luong, D.; Metcalfe, C.

- D.; Pawliszyn, J.; Servos, M. R. *Anal. Chem.* 2011, 83 (9), 3365–3370.
- (d) Zhang, X.; Oakes, K. D.; Luong, D.; Metcalfe, C. D.; Servos, M. R. *Anal. Chem.* 2011, 83 (17), 6532–6538.
- (2) (a) Walker, V.; Mills, G. A. *Ann. Clin. Biochem.* 2002, 39, 464–477. (b) Camel, V. *Spectrochim. Acta, Part B* 2003, 58 (7), 1177–1233.
- (3) Ouyang, G.; Vuckovic, D.; Pawliszyn, J. *Chem. Rev.* 2011, 111 (4), 2784–2814.
- (4) Pawliszyn, J. *Solid Phase Microextraction: Theory and Practice*; Wiley-VCH: New York, 1997.
- (5) Heringa, M. B.; Hermens, J. L. M. *Trends Anal. Chem.* 2003, 22 (9), 575–587.
- (6) Ulrich, S. *J. Chromatogr., A* 2000, 902 (1), 167–194.
- (7) Kramer, N. I.; van Eijkelen, J. C. H.; Hermens, J. L. M. *Anal. Chem.* 2007, 79 (18), 6941–6948.
- (8) (a) Chiap, P.; Rbeida, O.; Christiaens, B.; Hubert, P.; Lubda, D.; Boos, K. S.; Crommen, J. *J. Chromatogr., A* 2002, 975 (1), 145–155.
- (b) Mullett, W. M.; Pawliszyn, J. *Anal. Chem.* 2002, 74 (5), 1081–1087. (c) Musteata, M. L.; Musteata, F. M.; Pawliszyn, J. *Anal. Chem.* 2007, 79 (18), 6903–6911.
- (9) Musteata, F. M. *Clin. Chem.* 2006, 52 (4), 708–715.
- (10) (a) Zhang, X.; Es-haghi, A.; Musteata, F. M.; Ouyang, G.; Pawliszyn, J. *Anal. Chem.* 2007, 79 (12), 4507–4513. (b) Mirnaghchi, F. S.; Pawliszyn, J. *Anal. Chem.* 2012, 84 (19), 8301–8309.
- (11) Es-haghi, A.; Zhang, X.; Musteata, F. M.; Bagheri, H.; Pawliszyn, J. *Analyst* 2007, 132 (7), 672–678.
- (12) Zhou, S. N.; Zhang, X.; Ouyang, G.; Es-haghi, A.; Pawliszyn, J. *Anal. Chem.* 2007, 79 (3), 1221–1230.
- (13) Zhang, X.; Oakes, K. D.; Luong, D.; Metcalfe, C. D.; Pawliszyn, J. *Anal. Chem.* 2011, 83 (6), 2371–2377.
- (14) Ai, J. *Anal. Chem.* 1997, 69 (6), 1230–1236.
- (15) Zhou, S. N.; Zhao, W.; Pawliszyn, J. *Anal. Chem.* 2008, 80 (2), 481–490.
- (16) (a) He, J. H.; Liu, Y.; Xu, L. *Mater. Sci. Technol.* 2010, 26 (11), 1275–1287. (b) Arinstein, A.; Zussman, E. *J. Polym. Sci., Part B: Polym. Phys.* 2011, 49 (10), 691–707.
- (17) (a) Zewe, J. W.; Steach, J. K.; Olesik, S. V. *Anal. Chem.* 2010, 82 (12), 5341–5348. (b) Chigome, S.; Darko, G.; Torto, N. *Analyst* 2011, 136 (14), 2879. (c) Chigome, S.; Torto, N. *Anal. Chim. Acta* 2011, 706 (1), 25–36.
- (18) (a) Takei, Y. G.; Aoki, T.; Sanui, K.; Ogata, N.; Sakurai, Y.; Okano, T. *Macromolecules* 1994, 27 (21), 6163–6166. (b) Huber, D. L. *Science* 2003, 301 (5631), 352–354.
- (19) (a) Ivanov, A. E.; Ekeroth, J.; Nilsson, L.; Mattiasson, B.; Bergenstahl, B.; Galaev, I. Y. *J. Colloid Interface Sci.* 2006, 296 (2), 538–544. (b) Svetushkina, E.; Puretskiy, N.; Ionov, L.; Stamm, M.; Synytska, A. *Soft Matter* 2011, 7 (12), 5691–5696. (c) Yu, Q.; Li, X.; Zhang, Y.; Yuan, L.; Zhao, T.; Chen, H. *RSC Adv.* 2011, 1 (2), 262–269.
- (20) Kang, X.; Pan, C.; Xu, Q.; Yao, Y.; Wang, Y.; Qi, D.; Gu, Z. *Anal. Chim. Acta* 2007, 587 (1), 75–81.
- (21) (a) Alcidia-León, M. C.; Lucena, R.; Cárdenas, S.; Valcárcel, M. *Anal. Chem.* 2009, 81 (3), 1184–1190. (b) Tsai, W. H.; Huang, T. C.; Huang, J. J.; Hsue, Y. H.; Chuang, H. Y. *J. Chromatogr., A* 2009, 1216 (12), 2263–2269. (c) Qin, H.; Gao, P.; Wang, F.; Zhao, L.; Zhu, J.; Wang, A.; Zhang, T.; Wu, R. a.; Zou, H. *Angew. Chem., Int. Ed.* 2011, 50 (51), 12218–12221.
- (22) Chen, M.; Dong, M.; Havelund, R.; Regina, V. R.; Meyer, R. L.; Besenbacher, F.; Kingshott, P. *Chem. Mater.* 2010, 22 (14), 4214–4221.
- (23) Zhang, Y.; Huang, Z. M.; Xu, X.; Lim, C. T.; Ramakrishna, S. *Chem. Mater.* 2004, 16 (18), 3406–3409.
- (24) Muthiah, P.; Hoppe, S. M.; Boyle, T. J.; Sigmund, W. *Macromol. Rapid Commun.* 2011, 32 (21), 1716–1721.
- (25) Zhang, X.; Oakes, K. D.; Luong, D.; Wen, J. Z.; Metcalfe, C. D.; Pawliszyn, J.; Servos, M. R. *Anal. Chem.* 2010, 82 (22), 9492–9499.
- (26) (a) Levitt, M. A.; Sullivan, J. B., Jr.; Owens, S. M.; Burnham, L.; Finley, P. R. *Am. J. Emerg. Med.* 1986, 4 (2), 121–125. (b) Benet, L. Z.; Oie, S.; Schwartz, J. B. *Pharmacological Basis of Therapeutics*; McGraw Hill: New York, 1996. (c) Musteata, F. M.; Pawliszyn, J.;

Qian, M. G.; Wu, J. T.; Miwa, G. T. *J. Pharm. Sci.* **2006**, *95* (8), 1712–1722. (d) Zeng, X. L.; Lei, G. H.; Wei, Y. M. *Chin. J. Chromatogr.* **2007**, *25* (3), 348–352.